

Skyrme Crystal in bilayer and multilayer graphene

Yasuhisa Sakurai* and Daijiro Yoshioka

Department of Basic Science, The University of Tokyo, 3-8-1 Komaba, Tokyo 153-8902, Japan

(Dated: June 3, 2019)

Ground state of the two dimensional electron systems in Bernal bilayer and ABC-stacked multilayer graphenes in the presence of a strong magnetic field is investigated by Hartree-Fock approximation. Phase diagram of the systems are obtained, focusing on charge density wave states including states with vortices of valley pseudospins (called Skyrme crystal). The single electron states in these stacked graphene are given by two-component wave function. That of the first excited Landau level has a component same as the lowest Landau level of the ordinary two-dimensional electrons. Because of this localized wave function, skyrmion crystal has low energy in this first excited level up to four layers of graphene, when inter layer distance is assumed to be infinitesimal. At the same time, bubble crystals are suppressed, so the phase diagram is different from that of a single layer graphene.

PACS numbers: 73.21.-b, 73.22.Gk, 73.22.Pr

I. INTRODUCTION

Over the past decades, the conventional two-dimensional electron system (2DES) in semiconductor heterostructures in a strong magnetic field has been studied. It is found that electron-electron interaction brings various phases (e.g., fractional quantum Hall effect (FQHE) states^{1,2} and charge density wave (CDW) states³). Similarly, graphene⁴, a flat sheet of carbons with a honeycomb lattice exfoliated from a graphite in 2004⁵, is under intensive investigation as new 2DES whose electron has a valley degree of freedom (K, K') and a linear dispersion. Exhibition of FQHE^{6,7} and CDW^{8,9} states in the new 2DES has been expected, FQHE was recently observed in a single layer graphene (SLG)^{10,11}. Furthermore, few-stacked graphenes recently attract attention due to its intriguing properties: a tunable band structure by the number of layers and its stacking sequence, and a controllable band gap by a perpendicular electrical field^{12,13}.

We focus on Bernal bilayer and ABC-stacked multilayer graphenes, which have chiral electrons concentrated on outer layers in low-energy state. In this paper, the CDW ground state of the 2DES in bilayer graphene (BLG) and multilayer graphene (M -LG, $M \geq 3$) in a strong magnetic field is studied by Hartree-Fock approximation. As candidates of the ground state, electron (hole) Wigner crystal, electron (hole) bubble crystal, and Skyrme crystal are considered. Skyrme crystal is the state with a topological texture of valley pseudospins. It has the lowest energy around a filling $\nu = 1$ in SLG⁹. Our mean-field analysis predicts that valley Skyrme crystal also has low energy in BLG and M -LG ($M = 2, 3, 4$) at the first-excited Landau level when the interlayer distance d is assumed to be infinitesimal.

This paper is organized as follows. In the next section, we set up low-energy effective Hamiltonian in the presence of a magnetic field for SLG, BLG, and M -LG. Then, Hartree-Fock approximation is applied to the system of interacting electrons and self-consistent equations are derived. In Sec.III, CDW states are introduced, including Skyrme crystals (more properly, meron and meron pair crystal). As a preliminary calculation, the energy of a skyrmion (antiskyrmion) pair excitation at a $\nu = 1$ ferromagnetic state is evaluated and compared with

that of a separated particle-hole excitation to find the condition where Skyrme crystal has low energy. In Sec.IV, numerical results are presented at the Landau level where Skyrme crystal is expected. In Sec.V, the validity of the results and a relation to experiments are discussed.

II. MODEL

A. Single-particle State in a Magnetic Field

For a single layer graphene (SLG), the low-energy effective Hamiltonian around K valley is given by

$$\mathcal{H}_K^{SLG} = v_F(p_x\sigma_x + p_y\sigma_y), \quad (1)$$

which has electron with a linear dispersion^{4,14-19}. Here, v_F is Fermi velocity, σ_x and σ_y are Pauli matrices acting on sublattice (A, B) space. The Hamiltonian for the K' valley is the complex conjugate of Eq.(1). In a perpendicular magnetic field $\mathbf{B} = B\mathbf{e}_z$, using a magnetic ladder operator $a = (\pi_x - i\pi_y)l_B/\sqrt{2}\hbar$ ($\pi = \mathbf{p} - e\mathbf{A}$), the single-particle Hamiltonian is written as

$$\mathcal{H}_K^{SLG} = \frac{\sqrt{2}\hbar v_F}{l_B} \begin{pmatrix} 0 & a \\ a^\dagger & 0 \end{pmatrix}, \quad (2)$$

where $l_B = \sqrt{\hbar/eB}$ is magnetic length.

The eigenenergies are

$$E_N = \pm v_F \sqrt{2e\hbar BN}, \quad (N = 0, 1, \dots), \quad (3)$$

where a positive (negative) sign is taken as electron (hole) state. The corresponding eigenstates have the form

$$\Phi_{K,N,X}^{SLG}(\mathbf{r}) = \begin{cases} \frac{1}{\sqrt{2}} e^{-i\mathbf{K}\cdot\mathbf{r}} \begin{pmatrix} \phi_{N-1,X}(\mathbf{r}) \\ \pm \phi_{N,X}(\mathbf{r}) \end{pmatrix} & (N \geq 1) \\ e^{-i\mathbf{K}\cdot\mathbf{r}} \begin{pmatrix} 0 \\ \phi_{N,X}(\mathbf{r}) \end{pmatrix} & (N = 0) \end{cases}, \quad (4)$$

for K valley. In Landau gauge, $\phi_{N,X}(\mathbf{r})$ is given by

$$\phi_{N,X}(\mathbf{r}) = \left(\frac{1}{\sqrt{\pi} 2^N N! l_B L} \right)^{1/2} i^N e^{-i\frac{\mathbf{X}}{l_B} \cdot \mathbf{y} - \frac{(\mathbf{x}-\mathbf{X})^2}{2l_B^2}} H_N \left(\frac{x-X}{l_B} \right), \quad (5)$$

where L is the length of the system, $H_N(x)$ is Hermite polynomial, $X = k_y l_B^2$ is guiding center coordinate. A macroscopic number of states with different X are degenerated at one Landau level. A single-particle density on each sublattice $2\pi l_B^2 \phi_{N,X}^* \phi_{N,X}$ becomes broader as index N increases. The states with broad density induce a bubble CDW and lose the profit to form skyrmions (see Sec.III).

Bernal-stacked bilayer graphene (BLG) and ABC-stacked multilayer graphene (M -LG) have low-energy quasiparticles with a dispersion $E \propto p^M$, where $M (\geq 2)$ is the number of layers^{12,13,20,21}. In two adjacent layers, BLG and M -LG have interlayer hoppings t_\perp between the sublattice β in the lower layer and the sublattice α in the upper layer. In a magnetic field, the effective single-particle Hamiltonian for BLG and M -LG, which act on outermost layer (top, bottom) space, have the same form

$$\mathcal{H}_K^{M-LG} = \hbar\omega_M \begin{pmatrix} 0 & a^M \\ (a^\dagger)^M & 0 \end{pmatrix}, \quad (M \geq 2), \quad (6)$$

where off-diagonal components represent M -times hopping via high-energy states in inner layers. Its eigenenergy is

$$E_N = \pm \hbar\omega_M \sqrt{N(N-1) \cdots (N-M+1)}, \quad (7)$$

where $\hbar\omega_M = t_\perp (\sqrt{2}\hbar v_F / t_\perp l_B)^M \propto B^{M/2}$. At zero-energy, M Landau levels are degenerated. The corresponding eigenstate has the form

$$\Phi_{K,N,X}^{M-LG}(\mathbf{r}) = \begin{cases} \frac{1}{\sqrt{2}} \begin{pmatrix} \phi_{N-M,X}(\mathbf{r}) \\ \pm \phi_{N,X}(\mathbf{r}) \end{pmatrix} & (N \geq M) \\ \begin{pmatrix} 0 \\ \phi_{N,X}(\mathbf{r}) \end{pmatrix} & (N < M) \end{cases}, \quad (8)$$

for K valley. Notice that in the first excited state realized at $N = M$, the upper component of the wave function is given by $\phi_{0,X}(\mathbf{r})$, which is the ground state wave function of the ordinary 2-d electrons.

At Landau level $N < M$, the valley degree of freedom coincides with the layer degrees of freedom. If the layer degree of freedom in M -LG model is regarded as the sublattice degree of freedom, Eq.(8) is formally identical to that of SLG model when $M = 1$. In the following, the case of $M = 1$ ($M = 2$) represents the model of SLG (BLG).

B. The Hartree-Fock Hamiltonian

Although electron state is mainly considered in the following, hole state can be treated in the same way. In the present case of strong magnetic fields, electronic spins are completely polarized and the gap around the neutrality point is sufficiently large, then we take only one spin component and ignore the effect of Landau level transitions. Apart from a constant kinetic term, the Hamiltonian for interacting electrons in M -LG

($M \geq 1$) is given by

$$\mathcal{H}_{\text{int}} = \frac{1}{2} \int d^2 r dz \int d^2 r' dz' \sum_{\sigma_1, \sigma_2, \sigma_3, \sigma_4} \hat{\psi}_{M,N}^{\sigma_1 \dagger}(\mathbf{r}, z) \hat{\psi}_{M,N}^{\sigma_2 \dagger}(\mathbf{r}', z') \times V(|\mathbf{r} - \mathbf{r}'|, |z - z'|) \hat{\psi}_{M,N}^{\sigma_3}(\mathbf{r}', z') \hat{\psi}_{M,N}^{\sigma_4}(\mathbf{r}, z), \quad (9)$$

where the field operator $\hat{\psi}_{M,N}^\sigma(\mathbf{r}, z)$ is represented by

$$\hat{\psi}_{M,N}^\sigma(\mathbf{r}, z) = \sum_X \Phi_{\sigma,N,X}^{M-LG}(\mathbf{r}, z) \hat{c}_{N,X}^\sigma, \quad (10)$$

and Coulomb interaction is written as

$$V(\mathbf{r}, z) = \frac{e^2}{\epsilon \sqrt{r^2 + z^2}}. \quad (11)$$

Here, ϵ is the dielectric constant, $\sigma = \pm$ represents valley K and K' , respectively, $\hat{c}_{N,X}^\sigma$ is an annihilation operator of the electron at valley σ with guiding center X . A valley scattering term is relatively small when the cut-off $q_{\text{max}} \ll K$ is used^{8,9,22}, so we can ignore it as far as the CDW with magnetic length scale is concerned. (When $B = 10\text{T}$, magnetic length $l_B \sim 80\text{\AA}$ is bigger than a lattice constant $a = 1.42\text{\AA}$.) Then, the Hamiltonian in \mathbf{q} -space is written as

$$\mathcal{H}_{\text{int}} = \frac{1}{2L^2} \sum_{\mathbf{q}} \sum_{\sigma_1, \sigma_2} \sum_{\xi_1, \xi_2} V_{\xi_1, \xi_2}(\mathbf{q}) \rho_{\xi_1}^{\sigma_1}(-\mathbf{q}) \rho_{\xi_2}^{\sigma_2}(\mathbf{q}), \quad (12)$$

$$\rho_{\xi}^{\sigma}(\mathbf{q}) = \frac{1}{2} \sum_X e^{-iq_x X - \frac{1}{4} q^2 l_B^2} L_{N_{\sigma, \xi}}(q^2 l_B^2 / 2) \hat{c}_{N, X + \frac{1}{2} q_y l_B^2}^{\sigma \dagger} \hat{c}_{N, X - \frac{1}{2} q_y l_B^2}^{\sigma}, \quad (13)$$

$$V_{\xi, \xi'}(\mathbf{q}) = \begin{cases} \frac{2\pi e^2}{\epsilon q} & \xi = \xi' \\ \frac{2\pi e^2}{\epsilon q} e^{-qd} & \xi \neq \xi' \end{cases}, \quad (14)$$

where $L_n(x)$ is Laguerre polynomial, and $N_{\sigma, \xi}$ is defined by $N_{+, \uparrow} = N_{-, \downarrow} = N - M$ and $N_{+, \downarrow} = N_{-, \uparrow} = N$. The interaction between the electrons in different layers is weakened by a interlayer distance d , $d \sim 0.335\text{\AA}$ for BLG. When Landau level index N is smaller than the number of layers M , the valley degree of freedom coincides to that of layers (sublattices for SLG), and $\rho_{\uparrow}^+(\mathbf{r}) = \rho_{\downarrow}^-(\mathbf{r}) = 0$, $\rho_{\uparrow}^+(\mathbf{r})$ and $\rho_{\downarrow}^-(\mathbf{r})$ are twice the amount of eq.(13).

For the Hartree-Fock decoupling of \mathcal{H}_{int} , we assume the following order parameters

$$\Delta_N^{\sigma, \sigma'}(\mathbf{Q}) = \frac{2\pi l_B^2}{L^2} \sum_X \langle \hat{c}_{N, X+}^{\sigma \dagger} \hat{c}_{N, X-}^{\sigma'} \rangle e^{-i\mathbf{Q} \cdot \mathbf{X}}, \quad (15)$$

where \mathbf{Q} is a reciprocal lattice vector of the CDW state. Then the Hartree-Fock Hamiltonian is given by²³⁻²⁶

$$\mathcal{H}_{\text{HF}} = \sum_{\mathbf{Q}} \sum_X \sum_{\sigma \sigma'} H_{M,N}^{\sigma, \sigma'}(\mathbf{Q}) e^{-i\mathbf{Q} \cdot \mathbf{X}} \Delta_N^{\sigma, \sigma'}(-\mathbf{Q}) \hat{c}_{N, X+}^{\sigma \dagger} \hat{c}_{N, X-}^{\sigma'} - \sum_{\mathbf{Q}} \sum_X \sum_{\sigma \sigma'} X_{M,N}^{\sigma, \sigma'}(\mathbf{Q}) e^{-i\mathbf{Q} \cdot \mathbf{X}} \Delta_N^{\sigma, \sigma'}(-\mathbf{Q}) \hat{c}_{N, X+}^{\sigma \dagger} \hat{c}_{N, X-}^{\sigma}, \quad (16)$$

where $X_{\pm} = X \pm Q_y l_B^2/2$. The Hartree-Fock potential consists of a direct term

$$H_{M,N}^{\sigma,\sigma'}(Q) = \sum_{\xi,\xi'} H_{M,N}^{\sigma\xi,\sigma'\xi'}(Q), \quad (17)$$

$$H_{M,N}^{\sigma\xi,\sigma'\xi'}(Q) = \frac{1}{4} \frac{e^2}{\epsilon l_B} \frac{1}{Q l_B} \left(\delta_{\xi,\xi'} + (1 - \delta_{\xi,\xi'}) e^{-Qd} \right) \times L_{N_{\sigma\xi}}(Q^2 l_B^2/2) L_{N_{\sigma'\xi'}}(Q^2 l_B^2/2) e^{-Q^2 l_B^2/2}, \quad (18)$$

and an exchange term

$$X_{M,N}^{\sigma,\sigma'}(Q) = \sum_{\xi,\xi'} X_{M,N}^{\sigma\xi,\sigma'\xi'}(Q), \quad (19)$$

$$X_{M,N}^{\sigma\xi,\sigma'\xi'}(Q) = \frac{1}{4} \frac{e^2}{\epsilon l_B} \int_0^{\infty} dx \left(\delta_{\xi,\xi'} + (1 - \delta_{\xi,\xi'}) e^{-x d / l_B} \right) \times J_0(Q x l_B) e^{-\frac{1}{2} x^2} L_{N_{\sigma\xi}}\left(\frac{x^2}{2}\right) L_{N_{\sigma'\xi'}}\left(\frac{x^2}{2}\right). \quad (20)$$

Here, $J_n(x)$ is Bessel function of the first kind.

The real space density of electrons at valley σ and layer (sublattice) ξ is given by

$$\rho_{\xi}^{\sigma}(\mathbf{r}) = \frac{1}{2} \frac{1}{2\pi l_B^2} \sum_Q \Delta_N^{\sigma,\sigma'}(Q) L_{N_{\sigma\xi}}(Q^2 l_B^2/2) e^{iQ \cdot \mathbf{r} - Q^2 l_B^2/4}. \quad (21)$$

Filling factor at Landau level N is defined as

$$\nu_N = \frac{N_e}{N_{\phi}} \in [0, 2], \quad (22)$$

where $N_{\phi} = S/2\pi l_B^2$ (S is a area of the system) is degeneracy of Landau orbitals and N_e is the number of electrons. The factor 2 comes from the valley degree of freedom.

C. The Green Function Method

To determine the order parameters self-consistently, the Green function method is used^{8,9,24,25}. Single-particle Matsubara Green function is defined by

$$G_N^{\sigma,\sigma'}(X, X', \tau) = -\langle T c_{N,X}^{\sigma}(\tau) c_{N,X'}^{\sigma'\dagger}(0) \rangle. \quad (23)$$

The Fourier transformation

$$G_N^{\sigma,\sigma'}(Q, \tau) = \frac{2\pi l_B^2}{L^2} \sum_{X,X'} e^{-(i/2)Q_x(X+X')} \delta_{X,X'-Q_y l_B^2} G_N^{\sigma,\sigma'}(X, X', \tau), \quad (24)$$

relates to the order parameters $\Delta_N^{\sigma'\sigma}(Q)$ by

$$\Delta_N^{\sigma'\sigma}(Q) = G_N^{\sigma,\sigma'}(Q, \tau = 0^-). \quad (25)$$

Equation of motion for $G_N^{\sigma,\sigma'}(Q, \tau)$ is derived as

$$\begin{aligned} & \hbar(i\omega_n - \mu) G_N^{\sigma,\sigma'}(Q, \omega_n) - \hbar \delta_{Q,0} \delta_{\sigma,\sigma'} \\ &= \sum_{\sigma''} \sum_{Q'} \Sigma_{M,N}^{\sigma,\sigma''}(Q, Q') G_N^{\sigma'',\sigma'}(Q', \omega_n), \end{aligned} \quad (26)$$

from Heisenberg equation. Here, ω_n is Matsubara frequency for fermions, and the self-energy $\Sigma_{M,N}^{\sigma,\sigma'}(Q, Q')$ is given by

$$\begin{aligned} \Sigma_{M,N}^{\sigma,\sigma'}(Q, Q') &= \sum_{\sigma''} H_{M,N}^{\sigma''\sigma'}(|Q - Q'|) e^{-Q \times Q' l_B^2/2} \Delta_N^{\sigma'',\sigma'''}(Q - Q') \delta_{\sigma,\sigma'} \\ &\quad - X_{M,N}^{\sigma'\sigma}(|Q - Q'|) e^{-Q \times Q' l_B^2/2} \Delta_N^{\sigma',\sigma}(Q - Q'). \end{aligned} \quad (27)$$

To solve this self-consistent equation, we diagonalize the self-energy matrix

$$\sum_{Q'} \begin{pmatrix} \Sigma_{M,N}^{+,+}(Q, Q') & \Sigma_{M,N}^{+,-}(Q, Q') \\ \Sigma_{M,N}^{-,+}(Q, Q') & \Sigma_{M,N}^{-,-}(Q, Q') \end{pmatrix} \begin{pmatrix} V_j^+(Q') \\ V_j^-(Q') \end{pmatrix} = \gamma_j \begin{pmatrix} V_j^+(Q) \\ V_j^-(Q) \end{pmatrix}, \quad (28)$$

where (V_j^+, V_j^-) is j th eigenvector with eigenvalue γ_j . The order parameters are obtained from the eigenvectors and eigenvalues

$$\Delta_N^{\sigma\sigma'}(Q) = \sum_k f(\gamma_k - \mu) V_k^{\sigma'}(Q) V_k^{\sigma*}(0), \quad (29)$$

where $f(x)$ is Fermi-Dirac distribution function. The chemical potential μ is determined from

$$\sum_{\sigma} \Delta_N^{\sigma\sigma}(0) = \sum_{\sigma,j} V_j^{\sigma}(0) V_j^{\sigma*}(0) f(\gamma_j - \mu) = \nu_N. \quad (30)$$

Self-consistent equations are numerically calculated to yield the order parameters and the Hartree-Fock energy per particle for several CDW states introduced in Sec.III.

The order parameter sum rule at zero temperature²⁷, extended to the case of valley degeneracy

$$\sum_Q \sum_{\sigma'} |\Delta_N^{\sigma\sigma'}(Q)|^2 = \Delta_N^{\sigma\sigma}(0) = \nu_N^{\sigma}, \quad (31)$$

is easily derived from Eq.(29). Here, ν_N^{σ} is the contribution from valley σ electrons to the partial filling factor ν_N . This relation is used to check convergence of the results.

III. CHARGE DENSITY WAVE STATES

A. Valley Skyrmion

It is useful to map the valley degrees of freedom to a pseudospin⁹. In this language, the components of the pseudospin vector density $\mathbf{P}(Q) = P_x(Q)\hat{x} + P_y(Q)\hat{y} + P_z(Q)\hat{z}$ are defined by

$$P_x(Q) = \frac{\Delta_N^{+-}(Q) + \Delta_N^{-+}(Q)}{2}, \quad (32)$$

$$P_y(Q) = \frac{\Delta_N^{+-}(Q) - \Delta_N^{-+}(Q)}{2i}, \quad (33)$$

$$P_z(Q) = \frac{\Delta_N^{++}(Q) - \Delta_N^{--}(Q)}{2}. \quad (34)$$

In this paper, states with a topological pseudospin texture, which is called skyrmion²⁸, is considered. Skyrmion is a kind of spin texture usually used to describe a magnetic order, was first introduced in hadron physics²⁹. For conventional and SLG- 2DES, a state with aligned skyrmions, which is called Skyrme crystal, has been found around $\nu = 1$ ^{9,30}.

B. Preliminary consideration

Excitation energy of a skyrmion in a ferromagnetic uniform state at $\nu = 1$ is evaluated to find the conditions on which Skyrme crystal is preferred^{31,32}. When the interlayer distance $d \rightarrow 0$, the energy of a skyrmion (antiskyrmion) pair excitation Δ_{SK} and the energy of a widely separated particle-hole pair excitation Δ_{PH} are given by

$$\Delta_{SK} = \frac{1}{4\pi} \int_0^\infty q^3 V(q) [\mathcal{F}_{M,N}(q)]^2 e^{-q^2 l_B^2/2} dq, \quad (35)$$

$$\Delta_{PH} = \frac{1}{2\pi} \int_0^\infty q V(q) [\mathcal{F}_{M,N}(q)]^2 e^{-q^2 l_B^2/2} dq, \quad (36)$$

where the form factor $\mathcal{F}_{M,N}(q)$ has the form

$$\mathcal{F}_{M,N}(q) = \begin{cases} \frac{1}{2} \left[L_N \left(\frac{q^2 l_B^2}{2} \right) + L_{N-M} \left(\frac{q^2 l_B^2}{2} \right) \right] & (N \geq M) \\ L_N \left(\frac{q^2 l_B^2}{2} \right) & (N < M) \end{cases}. \quad (37)$$

The ratio of the two energies of the pair excitations is the same as that of single-particle excitations, from particle-hole symmetry. For conventional, SLG, BLG, and M -LG ($M = 3, 4, 5$) 2DESs, these energies at Landau level $N \leq 5$ are presented in Table I. It shows that skyrmion excitation is favored (1) at $N = 0$ in all systems as single-particle wave functions being identical to conventional one, (2) at $N = 1, 2, 3$ in SLG, and (3) at $N = M$ in M -LG ($M = 2, 3, 4$). Thus we can expect that the Skyrme crystal becomes the ground state in these situations around $\nu = 1$.

The reason why a skyrmion can be a low-energy excitation is the following³³. The ground state at $\nu = 1$ is a pseudospin ferromagnetic liquid state. When a hole is introduced in this state without flipping pseudospin of other electrons, the charge density of the hole is given by an eigenstate of the angular momentum, and is concentrated. On the other hand, when introduction of a hole is accompanied by pseudospin-flip of other electrons, many states with the same angular momentum are connected by the Coulomb interaction, and the charge density of the hole has wider distribution. This connected quantum state corresponds to a skyrmion. When the charge is confined like a wave function $\phi_{0,X}$ given by eq.(5), the formation of a skyrmion reduces the charge locality. At high Landau level N , however, a wave function $\phi_{N,X}$ is intrinsically broad, so the benefit to form skyrmions is lacking. In M -layered graphene, the spinor wave function has the localized component $\phi_{0,X}$ at Landau level $N = M$, so it can drive the system to form skyrmions.

TABLE I. Hartree-Fock quasiparticle and skyrmion (antiskyrmion) particle-hole excitation gaps (in unit of $e^2/\epsilon l_B \sqrt{\pi/2}$) at Landau level N for 2DES in a conventional semiconductor structure ($\Delta_{PH}^{conv.}$ and $\Delta_{SK}^{conv.}$), SLG (Δ_{PH}^{SLG} and Δ_{SK}^{SLG}), BLG (Δ_{PH}^{BLG} and Δ_{SK}^{BLG}), tri-LG (Δ_{PH}^{3-LG} and Δ_{SK}^{3-LG}), tetra-LG (Δ_{PH}^{4-LG} and Δ_{SK}^{4-LG}), and penta-LG (Δ_{PH}^{5-LG} and Δ_{SK}^{5-LG}). For conventional and SLG- 2DES, the energies of the two excitations were compared by Yang *et al.*³¹. The situation where the skyrmion is favored is emphasized by thick >.

N	$\Delta_{PH}^{conv.}$	$\Delta_{SK}^{conv.}$	Δ_{PH}^{SLG}	Δ_{SK}^{SLG}	Δ_{PH}^{BLG}	Δ_{SK}^{BLG}
0	1	> 1/2	1	> 1/2	1	> 1/2
1	0.75	< 0.875	0.6875	> 0.2188	0.75	< 0.875
2	0.6406	< 1.1328	0.5664	> 0.3301	0.5977	> 0.3770
3	0.5742	< 1.3418	0.5029	> 0.4097	0.5029	< 0.5151
4	0.5279	< 1.5522	0.4608	< 0.4754	0.4528	< 0.6181
5	0.4927	< 1.6834	0.4298	< 0.5328	0.4187	< 0.7048
N	Δ_{PH}^{3-LG}	Δ_{SK}^{3-LG}	Δ_{PH}^{4-LG}	Δ_{SK}^{4-LG}	Δ_{PH}^{5-LG}	Δ_{SK}^{5-LG}
0	1	> 1/2	1	> 1/2	1	> 1/2
1	0.75	< 0.875	0.75	< 0.875	0.75	< 0.875
2	0.6406	< 1.1328	0.6406	< 1.1328	0.6406	< 1.1328
3	0.5498	> 0.4448	0.5742	< 1.3418	0.5742	< 1.3418
4	0.4660	< 0.5808	0.5285	> 0.4870	0.5279	< 1.5522
5	0.4223	< 0.6829	0.4406	< 0.6284	0.4963	< 0.5390

C. The Crystal Structure

When Zeeman energy for valley pseudospins does not exist, a skyrmion splits into two merons (half-skyrmions). Four textures of a meron are possible from the two direction at center and the two vorticity. Charge density wave states where electrons, holes or merons form triangular or square lattice structure are considered. The order parameters $\Delta_N^{\sigma,\sigma'}(\mathbf{Q})$ are defined at points

$$\mathbf{Q} = \left[\left(j + \frac{1}{2}k \right) Q_0, \frac{\sqrt{3}}{2} k Q_0 \right], \text{ for a triangular lattice,} \quad (38)$$

$$\mathbf{Q} = (jQ_0, kQ_0), \text{ for a square lattice,} \quad (39)$$

where j and k are integers. The following states are assumed:

1. Electron Wigner crystal (eWC) and n -electron bubble crystal (eBCn); a triangular or square lattice with one or n electrons per unit cell. The fundamental length in \mathbf{q} -space Q_0 is determined from the condition that the CDW has n electrons in a unit cell: $\nu = 2\pi l_B^2 n/s$. Here, ν is filling factor of electrons and s is area of a unit cell. Low-energy state is pseudospin ferromagnetic because of Pauli principle.
2. Hole Wigner crystal (hWC) and n -hole bubble crystal (hBCn); a triangular or square lattice with one or n holes per unit cell. The fundamental length in \mathbf{q} -space Q_0 is determined from the condition that the CDW has n holes in a unit cell: $\nu_h = 2\pi l_B^2 n/s$. Here, ν_h is filling

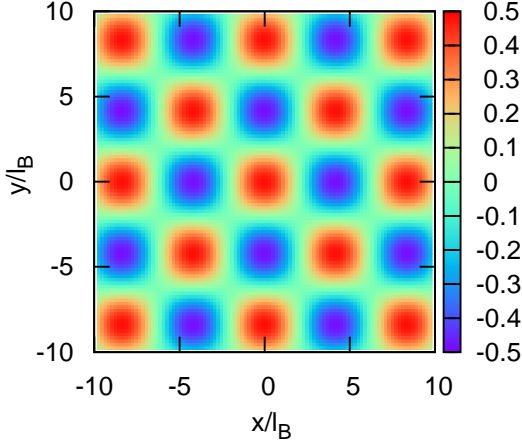


FIG. 1. (color online). $P_z(r)$ for meron crystal at $\nu_1 = 0.86$ in SLG.

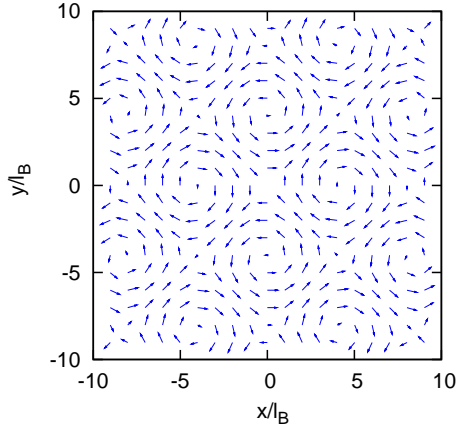


FIG. 2. (color online). The XY orientation of pseudospins for meron crystal at $\nu_1 = 0.86$ in SLG. One meron crystal has two types of merons.

factor of holes and s is area of a unit cell. Low-energy state is pseudospin ferromagnetic because of Pauli principle.

3. Meron crystal (MC); a square lattice with four merons of charge $-e/2$ ($\nu < 1$) or $e/2$ ($\nu > 1$) per unit cell, equally spaced. A meron pair is equivalent to one skyrmion, so MC can be seen as a state with two skyrmions per unit cell. Thus Q_0 is determined from the condition that the CDW has n ($= 2$) skyrmions in a unit cell: $\nu_h = 2\pi l_B^2 n/s$. The z component of pseudospin density in real space and the vorticity alternate from one site to the next (Fig.1, 2). The XY orientation of pseudospins has $U(1)$ symmetry (Fig. 2). The density distribution in real space is bipartite in layers.
4. Meron pair crystal (MPC); a triangular lattice with four merons per unit cell. The merons are not equally spaced and bound into pairs. The Q_0 is determined from the same way as MC. The energy of MPC is similar to MC, and have slightly lower energy in low quasiparticle-density regime (close to $\nu_N = 1$) in general.

IV. RESULTS

We use the partial filling factor ν_N at Landau level N , then the total filling factor is given by $\nu = 4N - 2 + \nu_N$ for any-layered graphene. Assume that Zeeman splitting is sufficiently large, so the phase diagram for $\nu_N \in [0, 2]$ is identical to that for $\nu_N \in [2, 4]$. Furthermore, the Hamiltonian has electron-hole symmetry around $\nu_N = 1$, so the phase diagram for $\nu_N > 1$ is caught by alternating particles for $\nu_N < 1$ to antiparticles. Numerical calculation for MC and MPC are done at $|1 - \nu_N| \geq 0.06$, since too many wave vectors are needed to get well-converged solutions at $\nu_N \approx 1$. In the following results, the energies with an accuracy of 10^{-6} are presented. Wigner and bubble crystals are calculated only in triangular symmetry, a square lattice generally has higher energy than a triangular one in a low quasiparticle-density regime.

It is difficult to get MC solutions close to $\nu_N = 1.0$, so we extrapolate the order parameters of the MC solutions in $\nu_N \leq 0.94$. To execute the extrapolation, the quantity $\mathcal{F}_{M,N}(Q)\Delta^{\sigma,\sigma'}(Q)$ is fitted by a quadratic curve. The energies of the extrapolated MC states are represented in the following figures as a dotted line. It is noted that uncertainty remains in the extrapolation especially in the 4-LG case. It comes from relatively low validity of the fitting the order parameters which have an inflection point near $\nu_N = 0.92$.

The energies of the valley-concentrated hole Wigner crystal states which are quite accurately approximated by Gaussian form order parameters

$$\begin{aligned} \Delta^{\sigma,\sigma}(0) &= \nu_N, \Delta^{\sigma,\sigma}(Q \neq 0) = (\nu_N - 1)e^{-Q^2 l^2/4}, \\ \Delta^{\sigma,\bar{\sigma}}(Q) &= \Delta^{\bar{\sigma},\sigma}(Q) = \Delta^{\bar{\sigma},\bar{\sigma}}(Q) = 0, \end{aligned} \quad (40)$$

are represented as 'GhWC' in the following figures in this chapter. In the vanishing interlayer distance limit, the GhWC state with $P_z = (\nu_N^+ - \nu_N^-)/2 = \pm \nu_N/2$ is degenerated to the hWC solutions with $|P_z| < \nu_N/2$ (Fig.4, 6, 8).

A. Single Layer Graphene

The Hartree-Fock (HF) phase diagram of the 2DES in SLG has been obtained and compared with that of the conventional one⁸. It is shown that Skyrme crystal (MC and MPC) become ground state around $\nu_N = 1$ at Landau level $N = 0$ and 1⁹. Considering the excitation energies for SLG (Table I), Skyrme crystal phase is also possible to occur at $N = 2$ and 3, but has not been found yet in a mean-field calculation. Although the same HF calculation had been done for SLG^{8,9}, we executed additional checks and investigated the higher-filling regime.

At Landau level $N = 0$, the phase diagram is the following: eWC for $\nu_0 \in [0.10, 0.50]$, hWC for $\nu_0 \in [0.50, 0.54]$, MC for $\nu_0 \in [0.54, 0.63]$, MPC for $\nu_0 \in [0.63, 0.92]$ ⁹.

At Landau level $N = 1$, the phase diagram is the following: eWC for $\nu_1 \in [0.10, 0.50]$, hWC for $\nu_1 \in [0.50, 0.73]$, MC for $\nu_1 \in [0.73, 0.84]$, MPC for $\nu_1 \in [0.84, 0.92]$ ⁹. The range of a skyrmionic (MC or MPC) phase is narrower than that of $N = 0$ case.

At Landau level $N = 2$, the phase diagram is the following: eWC for $\nu_2 \in [0.10, 0.27]$, eBC2 for $\nu_2 \in [0.27, 0.50]$, hBC2 for $\nu_2 \in [0.50, 0.73]$, hWC for $\nu_2 \in [0.73, 0.94]$. It's characteristic that 2-electron (hole) bubble crystals exist around $\nu_2 = 0.50$. Skymionic ground state is not seen in the range $\nu_2 \leq 0.94$. The extrapolating analysis, however, suggests that hWC and MC state are almost degenerated in $\nu_2 \in [0.94, 1.0]$.

At Landau level $N = 3$, the phase diagram is the following: eWC for $\nu_3 \in [0.10, 0.20]$, eBC2 for $\nu_3 \in [0.20, 0.30]$, eBC3 for $\nu_3 \in [0.30, 0.50]$, hBC3 for $\nu_3 \in [0.50, 0.70]$, hBC2 for $\nu_3 \in [0.70, 0.80]$, hWC for $\nu_3 \in [0.80, 0.94]$. Skymionic state does not appear in $\nu \leq 0.94$.

Although the MC and MPC solutions are not found in $\nu_N \leq 0.94$ for SLG at $N = 2$ and 3, Skyrme crystal is expected to have lower energy in the immediate vicinity of $\nu_N = 1$ from the analysis in III B.

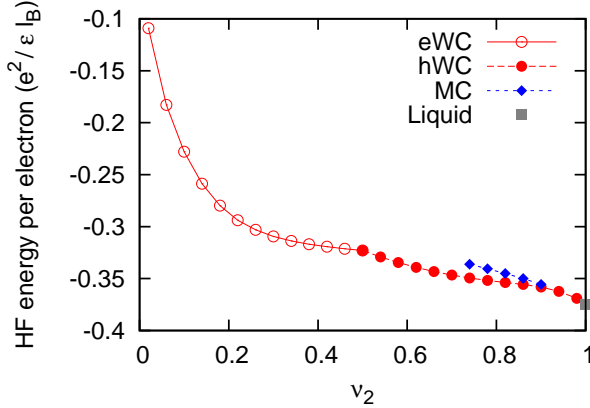


FIG. 3. (color online). Ground-state energy per particle (in units of $e^2/\epsilon l_B$) at Landau level $N = 2$ in BLG. ($d/l_B = 0$)

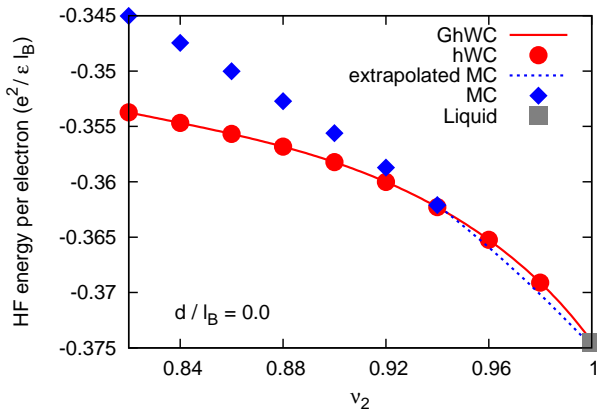


FIG. 4. (color online). Ground-state energy per particle (in units of $e^2/\epsilon l_B$) around filling $\nu_2 = 1$ at Landau level $N = 2$ in BLG. ($d/l_B = 0$)

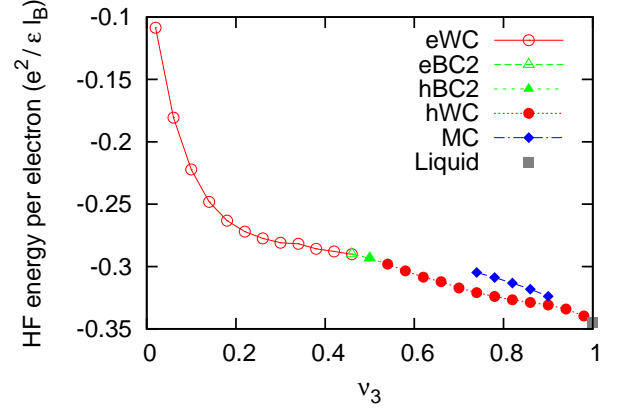


FIG. 5. (color online). Ground-state energy per particle (in units of $e^2/\epsilon l_B$) at Landau level $N = 3$ in tri-LG. ($d/l_B = 0$)

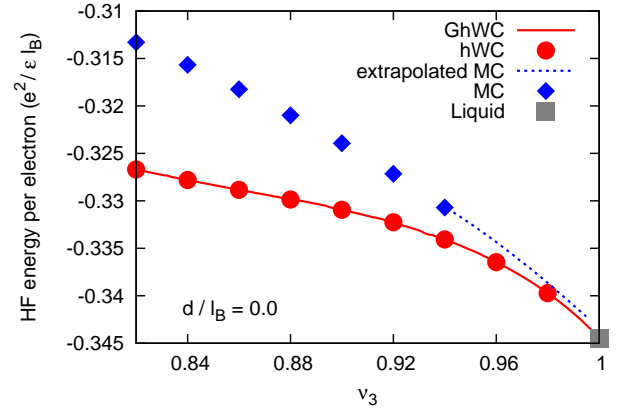


FIG. 6. (color online). Ground-state energy per particle (in units of $e^2/\epsilon l_B$) around filling $\nu_3 = 1$ at Landau level $N = 3$ in tri-LG. ($d/l_B = 0$)

B. Landau level $N = 2$ in Bilayer Graphene

The HF calculation for degenerated zero-energy Landau levels $N = 0, 1$ in BLG suggests the Skyrme crystal states of real spin or orbital-pseudospin occur³⁴.

In what follows, the results for the first-excited Landau level $N = 2$ in BLG are presented. For convenience, we first assume vanishing interlayer distance $d/l_B = 0$. Figure 3 shows the energies per electron for several crystal structures. It shows the following sequence of ground states: eWC for $\nu_2 \in [0.10, 0.50]$, hWC for $\nu_2 \in [0.50, 0.94]$. Bubble state does not appear unlike the phase diagram at Landau level $N = 2$ for SLG. Figure 4 shows the energies in the area close to $\nu_2 = 1$. The extrapolated energy of the MC solutions have lower value than hWC for $\nu_2 \in [0.94, 1.0]$.

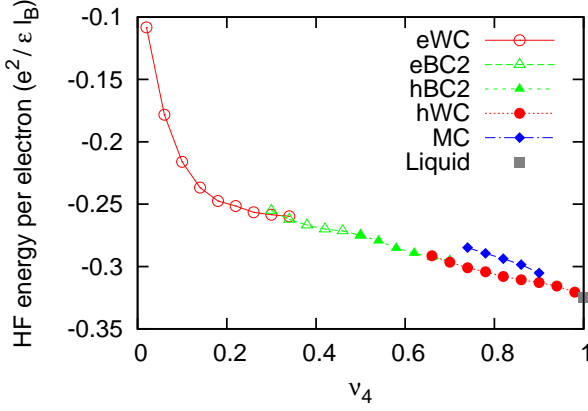


FIG. 7. (color online). Ground-state energy per particle (in units of $e^2/\epsilon l_B$) at Landau level $N = 4$ in tetra-LG ($d/l_B = 0$)

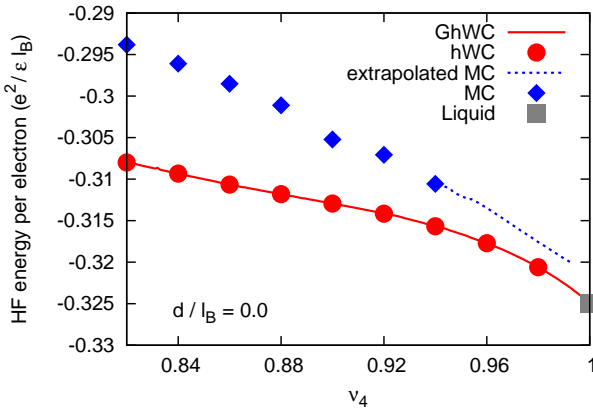


FIG. 8. (color online). Ground-state energy per particle (in units of $e^2/\epsilon l_B$) around filling $\nu_4 = 1$ at Landau level $N = 4$ in tetra-LG. ($d/l_B = 0$)

C. Landau level $N = 3$ in Trilayer Graphene

Figure 5 shows the energies per electron for several crystal structures at Landau level $N = 3$ in tri-LG, where $d/l_B = 0$ is assumed. It shows the following sequence of ground states: eWC for $\nu_3 \in [0.10, 0.46]$, eBC2 for $\nu_3 \in [0.46, 0.50]$, hBC2 for $\nu_3 \in [0.50, 0.54]$, hWC for $\nu_3 \in [0.54, 0.94]$. Although the bubble states are found around $\nu_3 = 0.50$, its range is narrower than that of $N = 3$ case in SLG. Skyrmonic ground state is not seen in the range $\nu \leq 0.94$. Figure 6 shows the energies near $\nu_3 = 1$. The extrapolated states of the MC solutions have the energy close to that of hWCs in the vicinity of $\nu_3 = 1$.

D. Landau level $N = 4$ for Tetralayer Graphene

Figure 7 shows the energies per electron for various crystal structures at Landau level $N = 4$ for tetra-LG, where $d/l_B = 0$ is assumed. It shows the following sequence of ground states: eWC for $\nu_4 \in [0.10, 0.32]$, eBC2 for $\nu_4 \in [0.32, 0.50]$, hBC2

for $\nu_4 \in [0.50, 0.68]$, hWC for $\nu_4 \in [0.68, 0.94]$. The bubble states are found in the broad range $\nu_4 \in [0.32, 0.68]$. Skyrmonic ground state is not seen in the range $\nu_4 \leq 0.94$. Figure 8 shows the energies near $\nu_4 = 1$. The extrapolated states of the MC solutions have higher energy than that of hWCs in the vicinity of $\nu_4 = 1$. As previously mentioned, however, the extrapolation method is no longer valid in tetra-LG. According to the analysis in III B, Skyrme crystal is expected to have the lowest energy in the vicinity of $\nu_4 = 1$.

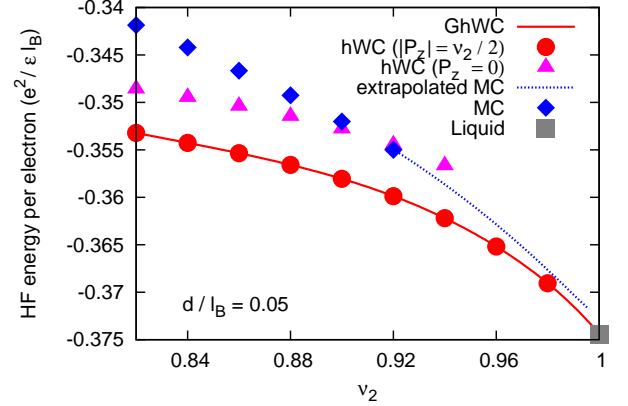


FIG. 9. (color online). Ground-state energy per particle (in units of $e^2/\epsilon l_B$) around filling $\nu_2 = 1$ at Landau level $N = 2$ in BLG. ($d/l_B = 0.05$)

E. The Finite Interlayer Distance

In reality, the interlayer distance is finite. When $d/l_B = 0.05$ for BLG ($B \sim 10$ T), the MC solutions and its extrapolated states always have higher energy than that of the Wigner crystal solutions polarized in the z -direction ($P_z = \pm \nu_N/2$) due to anisotropy of the pseudospin axis (Fig.9). The hWCs with $P_z = \pm \nu_N/2$ have unsymmetrical density distribution between the layers, and also have lower energy than that of the hWCs with $P_z = 0$. Similarly, the finite interlayer distance widens the gap between the MC and hWC ($P_z = \pm \nu_N/2$) energies in the other multilayer graphene systems.

V. DISCUSSION

The Hartree-Fock (HF) calculation suggests that (1) in the case of vanishing interlayer distance, meron crystal (MC) phase appears at Landau level $N = 2$ in BLG, and hole Wigner crystal (hWC) and MC states are degenerated around $\nu_N = 1$ at Landau level $N = 2$ in SLG, $N = 3$ in tri-LG, (2) in the case of a realistic interlayer distance, MC has higher energy than hWC with $P_z = \pm \nu_N/2$, which has unsymmetrical charge distribution between the layers. For the former case (1), our calculation strongly suggests that meron pair crystals (MPCs) will have lower energy in the immediate vicinity of $\nu_N = 1$ for its triangular symmetry. For the latter case (2), it's notable

that the possibility of other types of Skyrmonic crystals than MC and MPC remains.

Skyrme crystals (MC and MPC) have the charge distribution and the collective mode different from that of hWC, so these states can be distinguished by transport properties^{35,36} and a microwave absorption spectrum^{9,38}. Furthermore, the CDWs exist in outer layers, so the local density of states (LDOS) can be measured by spectroscopic manners³⁷. In this paper, unidirectional stripe phase is not considered. Stripe phase, however, also will appear around $\nu_N = 0.5$ in BLG and *M*-LG, as SLG⁸ and conventional 2DES if fractional quantum Hall states are not realized. Such a state, if exists, will be identified by anisotropic conduction³⁶.

Although we ignored the effects of disorder, a finite valley Zeeman energy, and Landau level transitions, it is unclear how these affect degeneracy of hWC and MC around $\nu_N = 1$. In particular, Landau level transitions in BLG and *M*-LG are larger than that of SLG under a magnetic field $B \sim 10$ T. The gap near a charge neutrality point is $\Delta_1 = \sqrt{2}\hbar v_F/l_B \sim 380\sqrt{B/\text{TK}}$ for SLG, $\Delta_2 = \sqrt{2}\hbar\omega_c \sim 45 \times (B/\text{T})\text{K}$ for BLG, $\Delta_3 = \sqrt{6}\hbar\omega_3 \sim 6.6 \times (B/\text{T})^{3/2}\text{K}$ for tri-LG, $\Delta_4 = \sqrt{24}\hbar\omega_4 \sim 1.1 \times (B/\text{T})^2\text{K}$ for tetra-LG. The typical Coulomb energy is

$E_C = e^2/\epsilon l_B \sim 100\sqrt{B/\text{TK}}$. For SLG, the ratio $E_C/\Delta_1 = 0.39$ is independent of field B . In this case it is shown that the Landau level mixing does not change the CDW phase diagram (except skyrmonic crystal)³⁹. For BLG and *M*-LG, high magnetic fields are needed to achieve the comparable ratio: $B \sim 70$ T for BLG, 60 T for tri-LG, 50 T for tetra-LG.

In HF approximation, charge ordered states are generally overestimated. However, it is known that HF calculation gives qualitatively correct results in a low quasiparticle-density regime such as near $\nu_N = 0$ and 1, according to comparisons with the results by the exact diagonalization method⁴⁰⁻⁴² or the density matrix renormalization group method⁴³. In this paper we focused on the possibility of meron crystals near $\nu_N = 1$, where only the competing states are Wigner crystals, i.e. one of the charge ordered states. Therefore, we think present results by the HF approximation is reliable.

ACKNOWLEDGMENTS

Y.S. thanks Prof. R. Côté for helping him to find self-consistent solution to MC states. The numerical calculation was done by SR11000 at Information Technology Center, The University of Tokyo.

* sakurai@toki.c.u-tokyo.ac.jp Your e-mail address

- ¹ D. C. Tsui, H. L. Stormer and A. C. Gossard, Phys. Rev. Lett. **48**, 1559 (1982).
- ² R. B. Laughlin, Phys. Rev. Lett. **50**, 1395 (1983).
- ³ H. Fukuyama, P. M. Platzman and P. W. Anderson, Phys. Rev. B **19**, 5211 (1979).
- ⁴ A. H. Castro Neto, F. Guinea, N. M. R. Peres, K. S. Novoselov and A. K. Geim, Rev. Mod. Phys. **81**, 109 (2009).
- ⁵ K. S. Novoselov, A. K. Geim, S. V. Morozov, D. Jiang, Y. Zhang, S. V. Dubonos, I. V. Gregorieva, and A. A. Firsov, Science **306**, 666 (2004).
- ⁶ V. M. Apalkov and T. Chakraborty, Phys. Rev. Lett. **97**, 126801 (2006).
- ⁷ N. Shibata and K. Nomura, J. Phys. Soc. Jpn. **78**, 104708 (2009).
- ⁸ C. H. Zhang and Y. N. Joglekar, Phys. Rev. B **75**, 245414 (2007).
- ⁹ R. Côté, J. -F. Jobidon, and H. A. Fertig, Phys. Rev. B **78**, 085309 (2008).
- ¹⁰ X. Du, I. Skachko, F. Duerr, A. Luican and E. Y. Andrei, Nature **462**, 192 (2009).
- ¹¹ K. I. Bolotin, F. Ghahari, M. D. Shulman, H. L. Stormer and P. Kim, Nature **462**, 196 (2009).
- ¹² H. Min and A. H. MacDonald, Phys. Rev. B **77**, 155416 (2008).
- ¹³ H. Min and A. H. MacDonald, Prog. Theor. Phys. Suppl. **176**, 227 (2008).
- ¹⁴ Wallace, Phys. Rev. **71**, 622 (1947).
- ¹⁵ J. C. Slonczewski and P. R. Weiss, Phys. Rev. **109**, 272 (1958).
- ¹⁶ G. W. Semenoff, Phys. Rev. Lett. **53**, 2449 (1984).
- ¹⁷ F. D. M. Haldane, Phys. Rev. Lett. **61**, 2015 (1988).
- ¹⁸ T. Ando, J. Phys. Soc. Jpn. **74**, 777 (2005).
- ¹⁹ N. M. R. Peres, F. Guinea, and A. H. Castro Neto, Phys. Rev. B **73**, 125411 (2006).
- ²⁰ J. Nilsson, A. H. Castro Neto, N. M. R. Peres and F. Guinea, Phys. Rev. B **73**, 214418 (2006).

- ²¹ E. McCann and V. I. Fal'ko, Phys. Rev. Lett. **96**, 086805 (2006).
- ²² M. O. Goerbig, R. Moessner, and B. Douçot, Phys. Rev. B **74**, 161407(R) (2006).
- ²³ R. Côté and A. H. MacDonald, Phys. Rev. Lett. **65**, 2662 (1990).
- ²⁴ R. Côté and A. H. MacDonald, Phys. Rev. B **44**, 8759 (1991).
- ²⁵ R. Côté, L. Brey and A. H. MacDonald, Phys. Rev. B **46**, 10239 (1992).
- ²⁶ X. M. Chen and J. J. Quinn, Phys. Rev. B **45**, 11054 (1992).
- ²⁷ D. Yoshioka and P. A. Lee, Phys. Rev. B **27**, 4986 (1983).
- ²⁸ R. Rajaraman, *Solitons and Instantons* (North-Holland, Amsterdam, 1982).
- ²⁹ T. H. R. Skyrme, Nucl. Phys. **31**, 556 (1962).
- ³⁰ L. Brey, H. A. Fertig, R. Côté and A. H. MacDonald, Surf. Sci. **361/362**, 274 (1996).
- ³¹ K. Yang, S. Das Sarma and A. H. MacDonald, Phys. Rev. B **74**, 075423 (2006).
- ³² K. Moon, H. Mori, K. Yang, S. M. Girvin, A. H. MacDonald, L. Zheng, D. Yoshioka and S. C. Zhang, Phys. Rev. B **51**, 5138 (1995).
- ³³ D. Yoshioka, *The Quantum Hall Effect* (Springer, 2002).
- ³⁴ R. Côté, Wenchen Luo, Branko Petrov, Yafis Barlas, and A. H. MacDonald, Phys. Rev. B **82**, 245307 (2010).
- ³⁵ V. J. Goldman, M. Santos, M. Shayegan and J. E. Cunningham, Phys. Rev. Lett. **65**, 2189 (1990).
- ³⁶ M. P. Lilly, K. B. Cooper, J. P. Eisenstein, L. N. Pfeiffer and K. W. West, Phys. Rev. Lett. **82**, 394 (1999).
- ³⁷ O. Poplavskyy, M. O. Goerbig, and C. Morais Smith, Phys. Rev. B **80**, 195414 (2009).
- ³⁸ H. Zhu, G. Sambandamurthy, Y. P. Chen, P. Jiang, L. W. Engel, D. C. Tsui, L. N. Pfeiffer, and K. W. West, Phys. Rev. Lett. **104**, 226801 (2010).
- ³⁹ C. H. Zhang and Y. N. Joglekar, Phys. Rev. B **77**, 205426 (2008).
- ⁴⁰ D. Yoshioka, B. I. Halperin and P. A. Lee, Phys. Rev. Lett. **50**,

1219 (1983).

- ⁴¹ D. Yoshioka, Phys. Rev. B **29**, 6833 (1984).
- ⁴² H. Wang, D. N. Sheng, L. Sheng and F. D. M. Haldane, Phys. Rev. Lett. **100**, 116802 (2008).
- ⁴³ N. Shibata and D. Yoshioka, Phys. Rev. Lett. **86**, 5755 (2001).